BOLETIN DE LA SOCIEDAD ESPAÑOLA DE
Cerámica y Vidrio
A R T I C U L O

Crystalline structure of the manganites solid solution RE(Me,Mn)O_3, (RE=Gd,Er; Me=Ni,Co)

C. MOURE[1], J. TARTAJ[1], A. MOURE[1], O. PEÑA[2]

[1]Electroceramics Department, Instituto de Cerámica y Vidrio, CSIC, 28049 Madrid, Spain
[2]Sciences Chimiques de Rennes, UMR 6226, Université de Rennes 1, 35042 Rennes, France

Estructura cristalina de las soluciones sólidas de manganitas RE(Me,Mn)O_3, (RE=Gd,Er, Me=Ni,Co)

Las propiedades estructurales de las soluciones sólidas RE(Me,Mn)O_3, RE=Gd,Er, Me=Ni,Co, han sido estudiadas por difracción de rayos X, (DRX) y medidas eléctricas. Las fases se sintetizaron por reacción en estado sólido entre los óxidos componentes. La incorporación de los cationes Ni^{2+} y $Co^{2+,3+}$ en la red en lugar de Mn lleva a cambios en los parámetros de red y en la simetría de la perovskita, $GdMnO_3$ o del compuesto hexagonal $ErMnO_3$ respectivamente. Las transiciones de fase dependen de la cantidad de Mn^{3+} sustituido, y por tanto de la debilitación del efecto co-operativo Jahn-Teller. Las soluciones sólidas basadas en $GdMnO_3$ cambian de perovskita tipo O' a perovskita tipo O. Esta transición ocurre para una menor cantidad de Ni que para Co como sustituyentes. Las soluciones basadas en $ErMnO_3$ muestran un comportamiento algo diferente: la incorporación induce cambios desde la estructura hexagonal a una estructura tipo perovskita en la forma O, para cantidades de ~20 at% Ni y para ~30 at% Co. La influencia del factor estérico en las transiciones observadas parece jugar un papel secundario frente a la desaparición progresiva de los cationes Jahn-Teller Mn^{3+}.

Palabras clave: manganitas, soluciones sólidas de perovskita, estructura cristalina, transiciones de fase.

The structural properties of the manganites solid solution RE(Me,Mn)O_3, RE=Er,Gd, have been studied by X-ray diffraction and electric measurements. Powders were prepared by solid state reaction between the component oxides. Incorporation of Ni^{2+} or Co^{2+} on the lattice in the Mn sites leads to changes in the parameters and symmetry of the perovskite or hexagonal compounds $GdMnO_3$ and $ErMnO_3$ respectively. The phase transitions depend on the amount of substituted Jahn-Teller Mn^{3+} cations, and, therefore, of the cooperative Jahn-Teller interaction weakness. Solid solutions based on $GdMnO_3$ perovskite compound change from O'-type to O-type orthorhombic perovskite symmetry when the Mn^{3+} cation amount decreases, because of the progressive substitution for Ni, Co. This transition occurs for lower amount of Ni^{2+} than for Co^{2+} cation. The Er-based solid solutions showed a different behaviour. For Ni^{2+} and Co^{2+} incorporation there are changes from hexagonal $ErMnO_3$-type lattice to perovskite-type symmetry, for 20 at% and 30 at% respectively of substituting cations. The resultant perovskites crystallised directly in the O-type orthorhombic perovskite structure. The steric influence seems to play a secondary role, such as it can be deduced of the small variation of the Goldschmidt tolerance factor, t, for perovskite structure.

Keywords: manganites; perovskite solid solutions; crystalline structure; phase transitions

1. INTRODUCTION

Rare-earth manganites $REMnO_3$ have focused a great lot of attention during the last decades due to their interesting properties in several fields of possible application.

Three issues are the cause of this interest for studying the manganite perovskites:

1º-Potential use of some manganites, such as $La_xSr_{1-x}MnO_{3-\delta}$ as cathodes for Solid Oxide Fuel cells, SOFC's, because of both electronic and ionic conductivity properties.

2º-Discovery of the colossal magnetic resistance phenomenon in compounds associated to lanthanum manganite.

Both issues are due to the appearance of a mechanism of double-change interaction between Mn^{3+} and Mn^{4+} that is induced by stoichiometric defects, vacancies, which are produced by means of partial substitution of trivalent cations,RE^{3+} or Mn^{3+} by divalent ones.

3º-Potential multiferroic features, which are bounded to the simultaneous appearance of a ferroelectric behaviour and an long-range antiferromagnetic order in some highly-anisotropic crystalline structures corresponding with the lower ionic radius RE cations, such as Y, Lu, Yb, and Er.

All these issues are related to the crystalline structure and the possible symmetries adopted by the rare-earth manganites, which are significatively different to those of other rare-earth $REMeO_3$ compounds, such as $REFeO_3$ ones.

The mixed oxides of general formula $REMeO_3$, where RE is a rare earth ion and Me=Fe, Cr, Ti, V, Rh, belong to the group of orthorhombic distorted perovskites, which crystallize in the space group (S.G.) Pbnm. When Me=Mn, the $REMnO_3$ compounds show the orthorhombic distorted perovskite structure only up to the Ho cation, whereas the compounds corresponding to RE with smaller ionic radii, from Er to Y, crystallize with a hexagonal-type structure and S.G. $P6_3cm$ (1).

As is well known, the distortion degree of the perovskite structure in ABO_3 compounds depends, between other causes, on steric effects, associated with changes in the ionic radius of the component A and B cations. This contribution is well represented by the Goldschmidt tolerance factor $t=(r_A+r_O)/(r_B+r_O)*\sqrt{2}$, where r_A represents the ionic radius of the large A cation (RE in the present case), r_B represents the ionic radius of the small B cation, (Fe, Cr, Mn, Ti, and others for the above-mentioned compounds), and r_O is the ionic radius of O^{2-}. When the tolerance factor decreases, the distortion degree increases (2). Nevertheless, in the case of the manganite compounds, $REMnO_3$, another factor must be considered with regard to the structure distortion. Thus, the Jahn-Teller nature of the Mn^{3+} cation induces an additional axial distortion effect, which is cooperative (3). Consequently, a combination of low t values and Jahn-Teller effect leads to a modification of the structure, from perovskite-type to the hexagonal-type structure mentioned above, with a higher grade of distortion with respect to the orthorhombic perovskites. Modifications in the crystalline structure of some manganites by formation of solid solutions $(RE,A)MnO_3$ in which A is a divalent cation such as Ba^{2+}, Sr^{2+}or Ca^{2+}, have been studied. The changes are more notorious in hexagonal manganites, which change to perovskite-type ones by adding an adequate amount of A cation, (4-6). Scarcer are works devoted to systematic study of the changes in the crystalline structure for incorporating Me^{2+} cations, such as Ni^{2+}, Co^{2+} or Cu^{2+}, on Mn sites forming solid solutions (7-9). Magnetic properties of some double perovskites RE_2MnMeO_6 are reported (10-12) but discussion about changes in the symmetry are not well developed.

In the present work the crystalline characteristics of solid solutions in four pseudo-binary oxides, based on the $REMnO_3$, RE=Gd,Er, modified by Ni^{2+} and Co^{2+}, are examined as a function of the nature of rare earth and transition metal cation. These compounds represent two different crystalline structural types, one, $GdMnO_3$ perovskite-type, and the $ErMnO_3$, hexagonal-type. Relationships between t, Mn^{3+} content, and phase transitions are discussed.

2. EXPERIMENTAL PROCEDURES

The samples have been prepared by solid state synthesis from the corresponding submicronic powder oxides Gd_2O_3, Er_2O_3, MnO., NiO and Co_3O_4 that were thoroughly wet mixed and homogenised by means of an attrition mill, with zirconia balls. The dried cake was repeatedly calcined and remilled for three times to assure a total reaction, with a thermal cycle of heating until 1150ºC, maintained 6h, and cooling down to room temperature. The heating and cooling rates were 5ºC/min and 1ºC/min respectively. The reacted products were characterised by X-Ray diffraction technique, and near pure perovskite phase was obtained for each composition. The cakes were remilled in an attrition ball mill. Fine, submicronic powder was uniaxilly pressed and late sintered at several temperatures. The samples were isothermally sintered under O_2 atmosphere, obtaining pure perovskite solid solutions in all the cases. The sintered, powdered samples were X-Ray diffraction, XRD, characterised by the Debye-Scherrer method, using a D-5000 Siemens Diffractometer with CuK_α radiation and Ni filter. The phases were identified using a scanning rate of 2º 2θ/min, and the lattice parameters were calculated from the spectra obtained on the sintered, grounded samples using a scanning rate of 1/8º 2θ/min. Si powder was employed as an internal standard. The lattice parameters were calculated using a mean square fits with all the peaks comprising between 2º and 75º 2θ angle range, (16-18 peaks), which have been indexed according to the S.G. Pbnm. Correlation coefficients >0.99 and standard deviation sum $<10^{-7}$ have been calculated for all the samples. The Goldschmidt tolerance

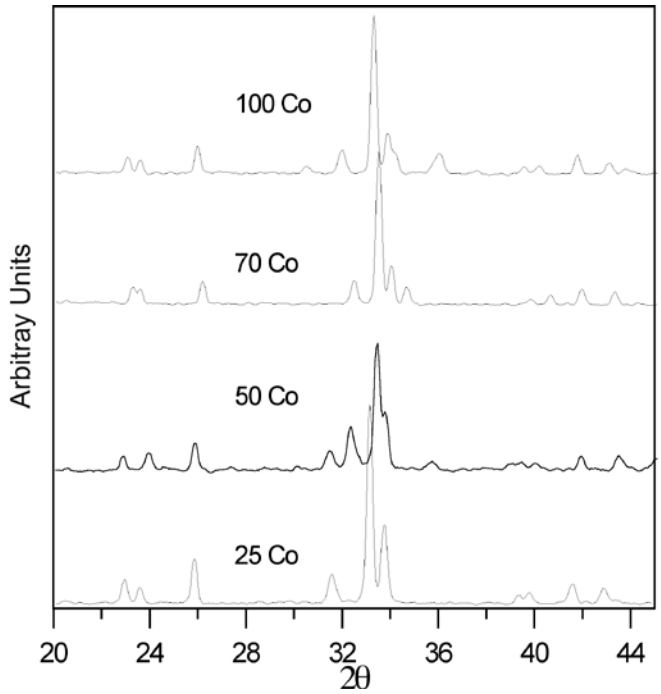

Figure 1. XRD patterns of $Gd(Co,Mn)O_3$ solid solutions, from 25 to 100 at% Co

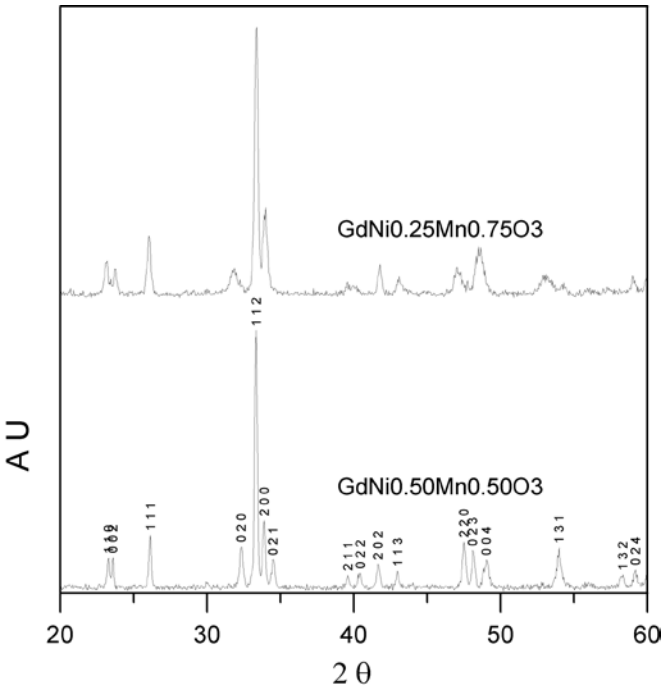

Figure 2. XRD patterns of $Gd(Ni,Mn)O_3$ solid solutions, from 25 to 50 at% Ni

factor t has been calculated using the ionic radii tabulated by Shannon (13), taking into account the oxygen coordination of the involved cations and the existence of different valence states of the Mn and the modifying cations, with different ionic radii, in the solid solutions. The mean ionic radius on *B* lattice sites has been used when two or more cations are present in them.

3. RESULTS AND DISCUSSION

Figures 1, 2, 3 and 4 show the XRD patterns of some representative solid solutions of the four systems. All the patterns have been well indexed as Pbnm orthorhombic perovskite-type crystalline structure and no secondary phases have been observed in the range of solid solutions studied for each system. Figures 5, 6, 7 and 8 show the evolution of the lattice parameters of the different solid solutions. In those ones, $c/\sqrt{2}$ has been represented in place of the c parameter for obtaining a higher clearness, thus showing the evolution from O'-type perovskite structure, ($c/\sqrt{2} \leq a \leq b$) to O-type one, ($a \leq c/\sqrt{2} \leq b$). Such as was stated for Y-based manganite solid solutions, (7), the progressive replacement of modifying cation, Ni, Co for Mn leads to a decrease of the lattice volume, which is more pronounced for Co incorporation that for Ni substitution. The decrease is also more pronounced from 50 at% to final of the series for Co replacement. Such as is known, pure $ErMnO_3$ crystallises with hexagonal-type structure, similar to that of $YMnO_3$ compound, with a S.G. $P6_3cm$. Solid solutions with Co, Ni lead to a change of symmetry from hexagonal to orthorhombic perovskite-type structure. It can be seen that the cation amount for which the transition takes place is higher for Co^{2+} cation than for Ni^{2+} one. On the other hand, the single-phase solid solution is extended far 50 at% for Co cation whereas with Ni cation, single-phase solid solution only is attained for $Ni^{2+} \leq 50$ at%, being biphasic samples those compositions with higher Ni amount. On the other hand, although $Gd(Co,Mn)O_3$ solid solutions are only represented from 25 to 100 at% Co, it must be say that the solid solution range between $GdMnO_3$ and $GdCoO_3$ compounds is total

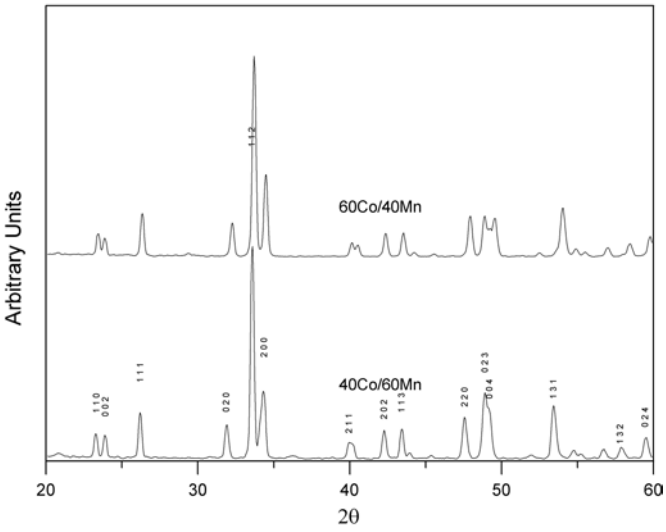

Figure 3. XRD patterns of $Er(Co,Mn)O_3$ solid solutions, for40 and 60 at% Co

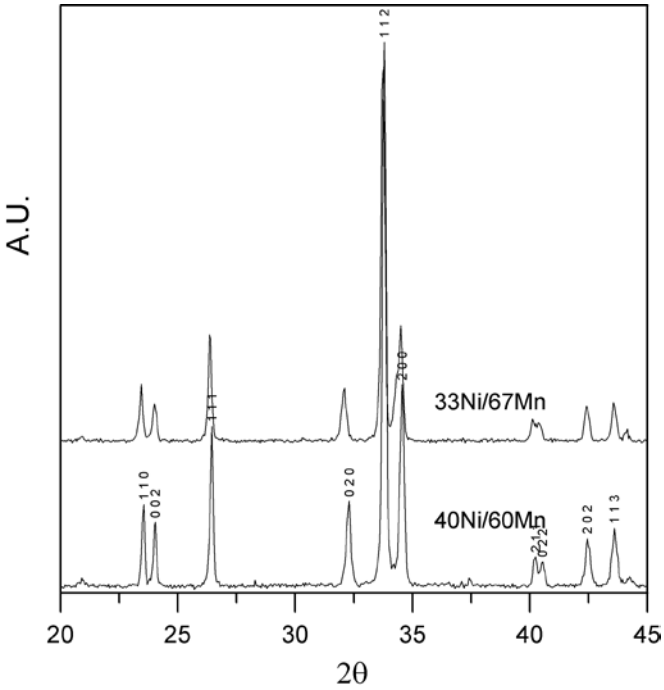

Figure 4. XRD patterns of $RE(Ni,Mn)O_3$ solid solutions, for 33 and 40 at% Ni

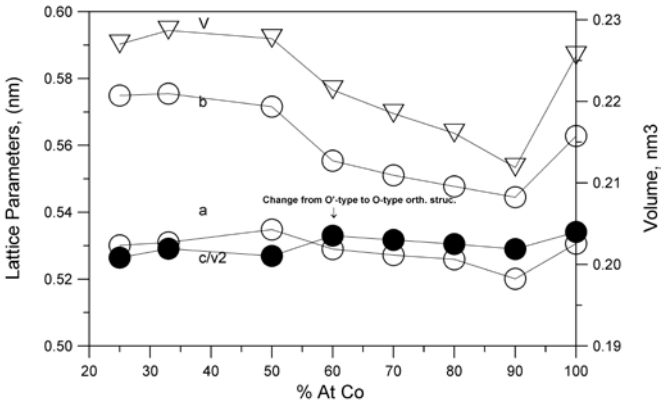

Figure 5. Lattice parameters vs at % Co for $Gd(Co,Mn)O_3$ solid solutions

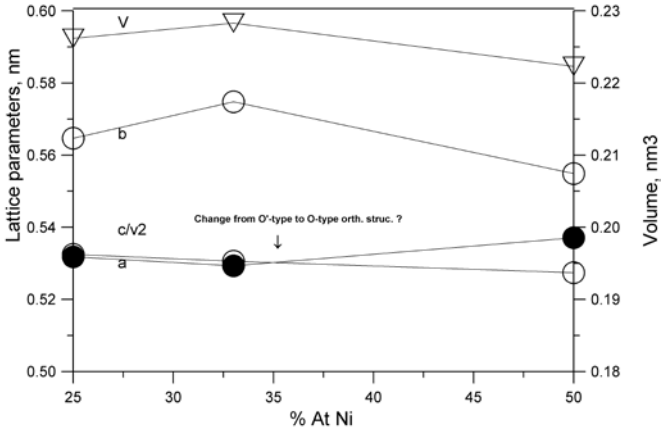

Figure 6. Lattice parameters vs at % Ni for $Gd(Ni,Mn)O_3$ solid solutions

between the two extremes. With Ni cation, the solid solution range only is attained for $Ni^{2+} \leq 50$ at%.

There are some differences between the solid solutions corresponding to the different rare-earth cations. Thus, the Gd-based solid solutions with Ni and Co cations always showed perovskite-type structure, parent of pure $GdMnO_3$, until 50 at% Ni-containing samples and until 100 at% Co, ($GdCoO_3$ crystallises with perovskite-type structure), such as corresponds to the stability of the Gd manganese perovskite structure. At the contrary of that reported by Farhoudi and Wang,(9) lattice parameters a and b decrease when Co rises from 50 to 90 at%, in a good correlation with the decrease of the B mean radius, such as is represented in figure 9. On the other hand, Er-based solid solutions showed the perovskite-type structure only from Ni or Co amounts above 20 or 30 at%, respectively, being biphasic samples those with lower doping contents, in which perovskite- and hexagonal-type coexist. Another difference is that the Er-based solid solutions, as well with Ni as with Co have orthorhombic O-type structure in all the existing perovskite solid solution range, see figures 7 and 8, whereas those Gd-based solid solutions show a transition from O'-type to O-type for an amount of modifying cation, which is higher for the Co cation than for the Ni cation, see figures 5-6. Finally, it is necessary to say as a last difference of Er-based solid solutions, with regard to Gd system, which was impossible to obtain pure perovskite-type samples for the $Er(Co,Mn)O_3$ solid solutions with Co amounts above 70 at%. Pure $ErCoO_3$ compound was not synthesised in the experimental conditions used in this work. Samples with Co>70at% showed a biphasic nature, with free Er_2O_3 and some traces of Co_3O_4, along with perovskite solid solutions with lattice parameters corresponding to Co amounts ≤70at%.

The reason for the different cation amount limit, which has been observed for Ni^{2+}-doping and Co^{2+}-doping, 20 and 30 at% respectively, which is needed for obtain perovskite-type samples from hexagonal $ErMnO_3$ can be attributed to the higher stability of the 2+ valence of Ni against Co, which could be in some extension in the form of Co^{3+}. Such as was stated elsewhere, (7), transition of hexagonal to perovskite-type structure is mainly due to progressive lowering of the Mn^{3+} amount in the lattice, and in a minor extension, to modification in the t tolerance factor, such as further will be discussed in this paper. Thus, if it is supposed that a small amount of Co^{3+} is formed, an equivalent part of Mn remains, as $Mn^{3+}$and, therefore, more amount of Co will be needed for causing the change from hexagonal to orthorhombic crystalline phase.

The observed decreasing of lattice parameters, Figures 7-8, when the doping cation amount rises, which are produced despite of the increase of the mean cationic radius by adding Co^{2+} and Ni^{2+}, with higher ionic radii than Mn^{3+}, (figure 10 and 11), and even taking into account that the incorporation of divalent cations leads to the appearance of equivalent amounts of Mn^{4+}, with lower ionic radius, only can be explained by the progressive disappearance of Jahn-Teller Mn^{3+} cations, and, therefore, of the cooperative distortion effect caused by the anisotropic structure of the external orbital (7).

The hypothesis that is established about the valence state of the doping cations is the following: for Co amounts ≤50 at% the valence state seems to be Co^{2+}, leading to the corresponding formation of an equivalent amount of Mn^{4+} to preserve the electroneutrality of the lattice. The B cation mean ionic radius must shows an increase. Effectively, the lattice volume grows but not in a significant mode. This is so probably due to the progressive disappearance of the Mn^{3+} John-Teller cations, which are the responsible of the strong lattice deformation that leads to an O'-type perovskite structure. It can be seen that for these Co amounts the tolerance factor decreases but the lattice symmetry slightly increases, see figure 5 and 7, $c/\sqrt{2}$ curve, which is then associated to that disappearance. Nevertheless, the symmetry of the solid solution is even orthorhombic O'-type. If the Co should be in the 3+ state, the B mean ionic radius must lower strongly because the ionic radius of LS Co^{3+} is lower than Mn^{3+}, and the Vegards'law would be accomplished.

In the $Gd(Mn,Co)O_3$ system for Co amounts ≥50 at% there is a strong decrease of the a and b lattice parameters and of lattice volume, thus indicating that Co^{3+} increases, lowering the B ionic mean radius and increasing the tolerance factor, with an appreciable rise of the lattice symmetry, represented by the $c/\sqrt{2}$ curve. The observed lattice parameters decreasing is indicating that the possible Co^{3+} cations are in the LS,

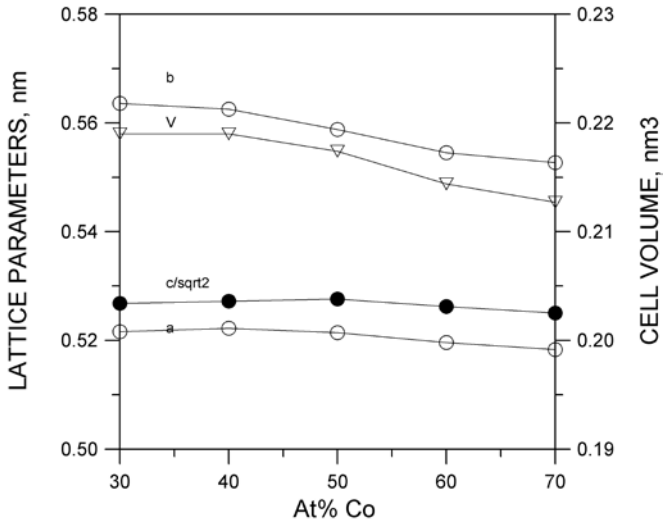

Figure 7. Lattice parameters vs at % Co for $Er(Co,Mn)O_3$ solid solutions

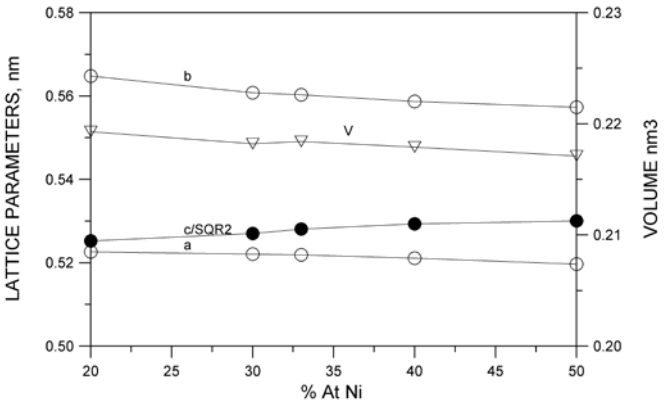

Figure 8. Lattice parameters vs at % Ni for $Er(Ni,Mn)O_3$ solid solutions

(low spin) state, for which the ionic radius is lower than the corresponding to the HS, (high spin) state. In this range is more difficult to establish what is the valence state of the Co cation, if is 3+ in whole, or if is partially 2+ and 3+. On the other hand, it can be seen that there is a transition from O' to O-type orthorhombic symmetry, i.e. the Mn is in whole in the 4+ valence state, such as is observed in the $Er(Ni_{0.5}Mn_{0.5})O_3$. in which Mn is in that 4+ valence state. This LS behaviour is seen as well in the Er-based solid solutions as in the Gd-based ones. The strong increase of the lattice parameters and volume that can be seen for pure $GdCoO_3$ is owing to the transition from LS to HS state of the Co^{3+} cation in this compound, such as was established by magnetic essays, (14).

Figures 9, 10, 11 are very illustrative of the change of symmetry. In the range of existing solid solution, mean B ionic radius grows, and, therefore t decreases. Nevertheless, the orthorhombic symmetry is maintained and $c/\sqrt{2}$ rises, (figure8), whereas the lattice volume lowers indicating a major lattice compaction and a minor deformation. This can be observed in both Er- and Gd-based solid solutions, see figures 6, and 8. In these figures it can be seen that the tolerance factor decreases when the cation increases, up to 50 at% of doping cation. Above this boundary value, for which it can be expected that all the Mn is in the form of Mn^{4+} the tolerance factor increases. Despite of the decrease in the t value, in the first region of the curve, the perovskite structures are fully formed and them trends towards a more symmetrical form. The presence or absence of Mn^{3+} Jahn-Teller cations plays, therefore, a fundamental role for determining the perovskite symmetry, whereas the steric factor represented by the tolerance factor plays a secondary rol. If are compared the values of t corresponding to the Er-based solid solutions with Ni and Co, one can be seen that, despite of the lower t value for Ni-containing compounds, formation of pure perovskite structure is attained at lower amounts of Ni, (20 at%), than that needed for stabilising the perovskite phase in the Co-containing system.

Table 1 resumes some results of conductivity measurements, performed at room temperature for Co amounts ≥50 at% in the $Gd(Mn,Co)O_3$ system. As it can be seen, conductivity increases with the Co content, indicating that there exist at least two valence states for Co, 2+ and 3+. If all the Co would be as 3+, and therefore, the Mn as 3+, the Jahn-Teller still should have some influence, and conductivity should be stable or decreasing. Increase of Co leads to an increase of the pairs Co^{3+}-Co^{2+} and the corresponding charge carriers.

The exposed model can be applied to the other solid solutions. Wider studies published elsewhere, (15) corroborate the model for Er-based solid solutions.

4. CONCLUSIONS.

The incorporation in solid solution of small divalent cations, Ni and Co, substituting for Mn in the hexagonal $ErMnO_3$ compound and in the perovskite-type $GdMnO_3$ compound, leads to a phase transitions in which a perovskite-type structure is formed from the hexagonal phase, or to a change from O'-type to O-type perovskite structure from the $GdMnO_3$ compound. The amount of substituting cation necessary for such transitions depends on the cation nature and less on the ionic radius. Cation with very stable (II)

TABLE 1. ELECTRICAL CONDUCTIVITY OF SOME SELECTED SOLID SOLUTIONS

Sample	S*cm^{-1}
$GdCo_{0.6}Mn_{0.4}O_3$	0.637
$GdCo_{0.7}Mn_{0.3}O_3$	2.55
$GdCo_{0.8}Mn_{0.2}O_3$	6.55
$GdCo_{0.9}Mn_{0.1}O_3$	8.04
$GdCo_{1.0}Mn_{0.0}O_3$	6.82

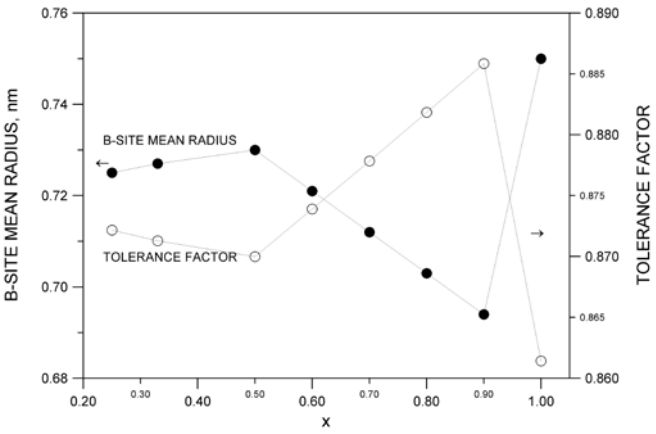

Figure 9. $Gd(Co,Mn)O_3$, tolerance factor and B-site mean ionic radius as a function of at % Co

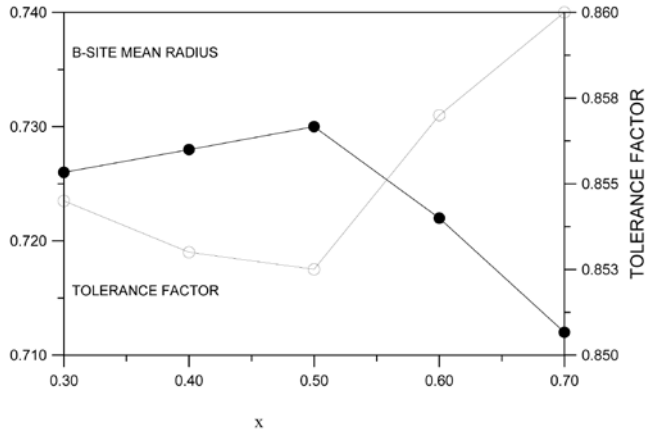

Figure 10. $Er(Co,Mn)O_3$, tolerance factor and B-site mean ionic radius as a function of at % Co

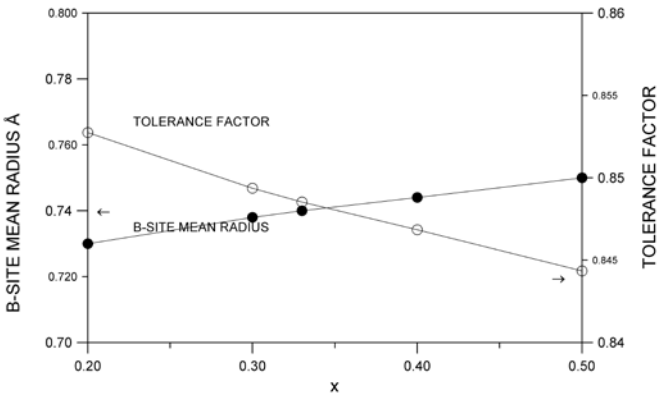

Figure 11. $Er(Ni,Mn)O_3$, tolerance factor and B-site mean ionic radius as a function of at % Ni

valence state, such as Ni^{2+} shows an upper limit to solid solution formation, which has been established at 50 at %. For variable-valence Co^{2+} Co^{3+} the solid solution limits is extended up to 70 at% for Er-based compounds and for the whole range, 100 at% for Gd-based compounds. The phase transition depends strongly on the progressive substitution of the Jahn-Teller Mn^{3+} cation, and therefore of the cooperative interaction weakness. The steric influence, represented by the tolerance factor, t, plays a secondary role, as is shown by the very slow variation of the tolerance factor, t, as a function of the cation content.

Electrical measurements have been carried out for corroborating the valence balance of the different cations involved in the solid solution formation. $Gd(Co,Mn)O_3$ solid solution shows electrical conductivity, which rises with the Co amount.

5. REFERENCES

1. O. Muller and R. Roy, *in* &&The Major Ternary Structural Families," pp. 357-358. Springer-Verlag, New York, 1974.
2. V. M. Goldschmidt, The laws of crystal chemistry, *Naturwissenschaften* 14, 477-485 (1926).
3. J. Rodrıiguez-Carvajal, M. Hennion, F. Moussa, and A. H. Moudden, Neutron-diffraction study of the Jahn-Teller transition in stoichiometric $LaMnO_3$, Physical Review B, 57, R3189, (1998)
4. C. Moure, M. Villegas, J. F. Fernández, J. Tartaj, P. Durán. Phase transition and electrical conductivity in the system $YMnO_3$-$CaMnO_3$. Jour. Mater. Sci 34,2565-2568, (1999)
5. C. Moure, D. Gutierrez, J.F. Fernandez, J. Tartaj, P. Duran, O. Peña, Phase transitions induced on hexagonal manganites by the incorporation of aliovalent cations on A or B lattice sites, Bol. Soc. Esp. Ceram. Vidr., 38, 417-420, (1999).
6. D. Vega, G. Polla, A. G. Leyva, P. Koning, H. Lanza, A. Esteban, H. Aliaga, M. T. Causa, M. Tovar, and B. Alascio, Structural Phase Diagram of $Ca_{1-x}Y_xMnO_3$: Characterization of Phases, *J. Solid State Chem*. 156, 458-463 (2001).
7. C. Moure, D. Gutierrez, O. Peña, P. Duran, Structural Characterization of $YMe_xMn_{1-x}O_3$ (*Me*=Cu, Ni, Co) *Journal of Solid State Chemistry* 163, 377-384, (2002)
8. Filonova EA, Cherepanov VA, Voronin VI, A study of the phase composition and crystal structure in the series of $LaCo_{1-x}Mn_xO_3$ +/-delta solid solutions, Zhurnal Fizicheskoi Khimii, 72, 10, 1876-1878,(1998)
9. M. Mehdi Farhoudi and X. L. Wang, Structure, Spin Glass, and Spin State in PerovskiteGd$Co_{1\,x}Mn_xO_+$ (x 0:5), IEEE Transactions on Magnetics, 41, 10, 3493-3495, (2005)
10. Kyomen T, Yamazaki R, Itoh M., Correlation between magnetic properties and Mn/Co atomic order in $LaMn_{0.5}Co_{0.5}O_{3+delta}$. 2. Magnetic and calorimetric properties. Chemistry of Materials, 16, 1, 179-184 (2004)
11. X.L. Wang, J. Horvat, H.K. Liu, A.H. Li, S.X. Dou, Spin glass state in Gd_2CoMnO_6 perovskite manganite, Solid State Communications 118, 27-30, (2001)
12. A. P. Sazonov, I. O. Troyanchuk1, V. V. Sikolenko, H. Szymczak, and K. Bärner, Effect of the oxygen nonstoichiometry on the structure and magnetic properties of Nd_2CoMnO_{6+d} double perovskites, Phys. stat. sol. (b) 244, 9, 3367–3376 (2007)
13. R. D. Shannon, Revised Effective Ionic Radii and Systematic Studies of Inter-atomic Distances in Halides and Chalcogenides, *Acta Crystallogr. A* 32, 751 (1976).
14. O. Peña, A.B. Antunes, G. Martínez, V. Gil, C. Moure, Inter-network magnetic interactions in $GdMe_xMn_{1-x}O_3$ perovskites (Me =transition metal), *Journal of Magnetism and Magnetic Materials* 310, 159 (2007)
15. O. Peña, A.B, Antunes, Baibich, M.N. Lisboa-Filho, P.N. Gil, V. Moure, C. Spin reversal and magnetization jumps in $ErMe_xMn_{1-x}O_3$ perovskites, (Me =Ni, Co), *Journal of Magnetism and Magnetic Materials* 312, 78, (2007)

Recibido: 6-4-09
Aceptado: 15-6-09